Globular surface layer in electron beam powder-bed fusion Ti-6Al-4V after standard powder removal blasting and hot isostatic pressing

Nicholas Derimow[1]*, Jake T. Benzing[1], Keenan Hanson[2], Nikolas Hrabe[1]

[1]*Applied Chemicals and Materials Division, NIST, 325 Broadway, Boulder, CO 80305, USA*

[2]*Stryker, Mahwah, NJ 07430 USA*

Abstract

A globular α recrystallization has been discovered at the surface of net shape electron beam powder-bed fusion (PBF-EB) Ti-6Al-4V alloy parts. This recrystallization is the result of powder recovery blasting followed by hot isostatic pressing treatment (HIP), which mimics the thermomechanical treatment necessary to achieve globularization in wrought Ti-6Al-4V. The thickness of the globular surface α is variable depending on the blasting intensity as well as the presence of surface protrusions that block the line-of-sight of the blasting media. The globular layer contains a {0001} orientation relationship parallel to the blasting direction, plus a low intragranular orientation deviation, when compared to the bulk. The results indicate that this globular α at the surface may be present for all net-shape Ti-6Al-4V components that have been manufactured via PBF-EB and subjected to a HIP treatment. Tunable fatigue and wear performance may be possible through controlled blasting parameters and globular surface layer thickness.

Keywords: Additive Manufacturing, Ti-6Al-4V, Powder Recovery, Recrystallization, Hot isostatic pressing

1. Introduction

The additive manufacturing (AM) of Ti-6Al-4V has been a steadily growing with applications in the biomedical [1] and aerospace sectors [2]. In electron beam powder-bed fusion (PBF-EB), the powder that encapsulates the part within the powder bed has been sintered due to the high processing temperature. Removing the sintered powder requires exposing the part to powder blasting. This process utilizes the feedstock powder from the PBF-EB process in a blast cabinet. Commonly in PBF-EB Ti-6Al-4V, the as-built part is subjected to a sub-β transus hot isostatic pressing (HIP) treatment in order to be service-ready for a desired application, such as Class C components as prescribed in ASTM F2924-14 [3]. The application

*Corresponding author
Email address: `nicholas.derimow@nist.gov` (Nicholas Derimow[1])

of HIP treatments to PBF-EB Ti-6Al-4V parts have been shown to reduce internal porosity [4], lengthen fatigue life [5], improve fatigue endurance ratio [6], and retain as-built strengths [7]. In many production environments, the part retrieval process followed by HIP are qualified steps in preexisting work flow. Since powder blasting is similar to shot peening, the aim of this work is to investigate whether any microstructural changes occur from this blasting process. This work will also look at the effects from the subsequent HIP process.

2. Methods

Cuboids were built using an Arcam Q10+[1] with standard build theme (software version 5.2.52) and a 50 µm layer height. The powder was plasma atomized Ti-6Al-4V with particle size range of 40 µm to 100 µm. All cuboids were built on the same build plate. Geometry is shown in Fig. 1. The cuboids were subjected to controlled blasting intensity in the blast cabinet during the powder removal. The blasting intensities were defined as Low = 420 mm working distance (WD) for 26 s, Medium = 150 mm WD for 26 s, and High = 50 mm WD for 53 s. An ultrasonic process was used to retrieve the non-blasted cuboid from the sintered powder. The HIP cycle (conforming to ASTM F2924 [3]) was greater than 100 MPa, 895°C to 955°C, held for 2 h and cooled in Ar to below 425 °C. There were 8 cuboid conditions studied in this work: No blast, No blast + HIP, Low Blast, Low Blast + HIP, Medium Blast, Medium Blast + HIP, High Blast, and High Blast + HIP.

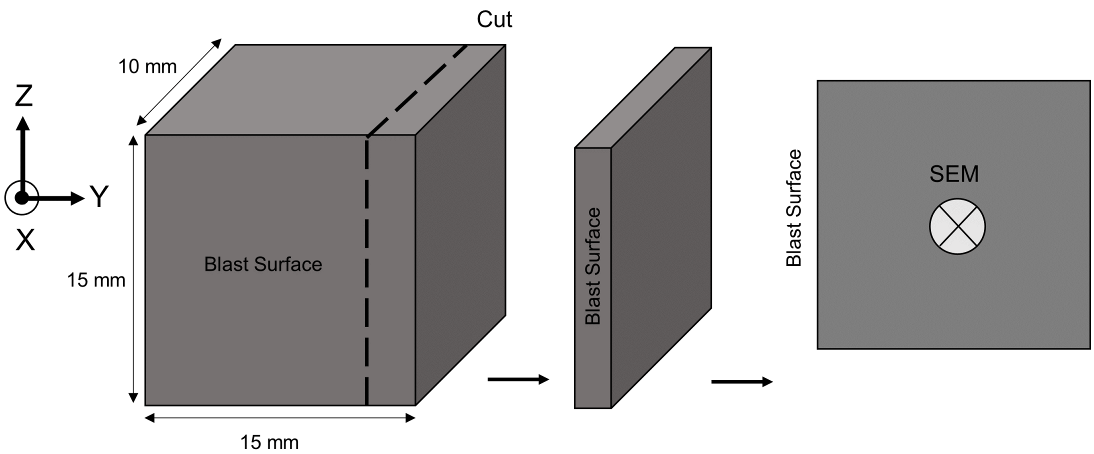

Figure 1: Flow detailing how the surface perpendicular to the powder blasting direction was imaged. X = blasting direction, Y = SEM beam direction, Z = build direction.

[1]Commercial names are identified in order to specify the experimental procedure adequately. This does not imply recommendation or endorsement by NIST nor does it imply that they are necessarily the best available for the purpose.

Metallographic specimens were mounted and polished down to 1 μm, followed by vibratory polishing for 24 h in 0.05 μm colloidal silica. The microstructures were imaged using a field emission scanning electron microscope (FE-SEM) equipped with a backscattered electron (BSE) detector using an accelerating voltage of 15 kV. Crystallographic information was obtained via electron backscatter diffraction (EBSD) on the same FE-SEM using an accelerating voltage of 20 kV and step size of 0.30 μm.

3. Results

The BSE images of the as-built specimens are presented in Fig. 2. The coordinate system for all micrographs and EBSD is such that X = blasting direction, Y = SEM beam direction, and Z = build direction. The surface of the No- and Low-blasted specimens in Fig. 2a–b display jagged surface protrusions and partially bonded particles. The surfaces of the Med- and High-blasted specimens in Fig. 2c–d are flatter, with indications of plastic deformation (a change in BSE contrast [8]) near previously protruded regions, with sharp thin voids near the surface. The microstructure outside of the plastic deformation zone is the same for all as-built conditions, consisting of Widmänstatten $\alpha + \beta$ with fine α-laths (approx. 0.64 μm average thickness).

The BSE images of the HIP specimens are presented in Fig. 3 at equal magnifications to those in Fig. 2. There is Widmänstatten at the surface in the No-blast/HIP condition in Fig. 3a, however, observable surface globularization in the remaining HIP conditions in Fig. 3b–d. The thickness of the globular surface layer increases with increasing blasting intensity. In the areas where there was no line-of-sight contact from the powder blasting with the surface, there is no globular α present. The High-blast/HIP specimen shown in Fig. 3d has a visually smoother surface than the No/Low/Med-HIP specimens, with more continuous transformed globular α phase. The microstructure outside the globular surface layer is the same for all HIP conditions and is coarser (α-lath thickness approximately 2.00 μm) compared to the as-built conditions.

Crystallographic information for the High-blast/HIP specimen is shown in Fig. 4. The IPF map is oriented in the X direction. Fig. 4b is a grain reference orientation deviation (GROD) map of the same region. Figs. 4c–d are inverse pole figures showing the crystallographic texture of the two different regions of the globular surface α and internal Widmänstatten α, respectively. The surface globular α has stronger $\{0001\}_\alpha$ texture whereas the internal texture is more closely oriented in the $\{2\bar{1}\bar{1}0\}_\alpha$ direction.

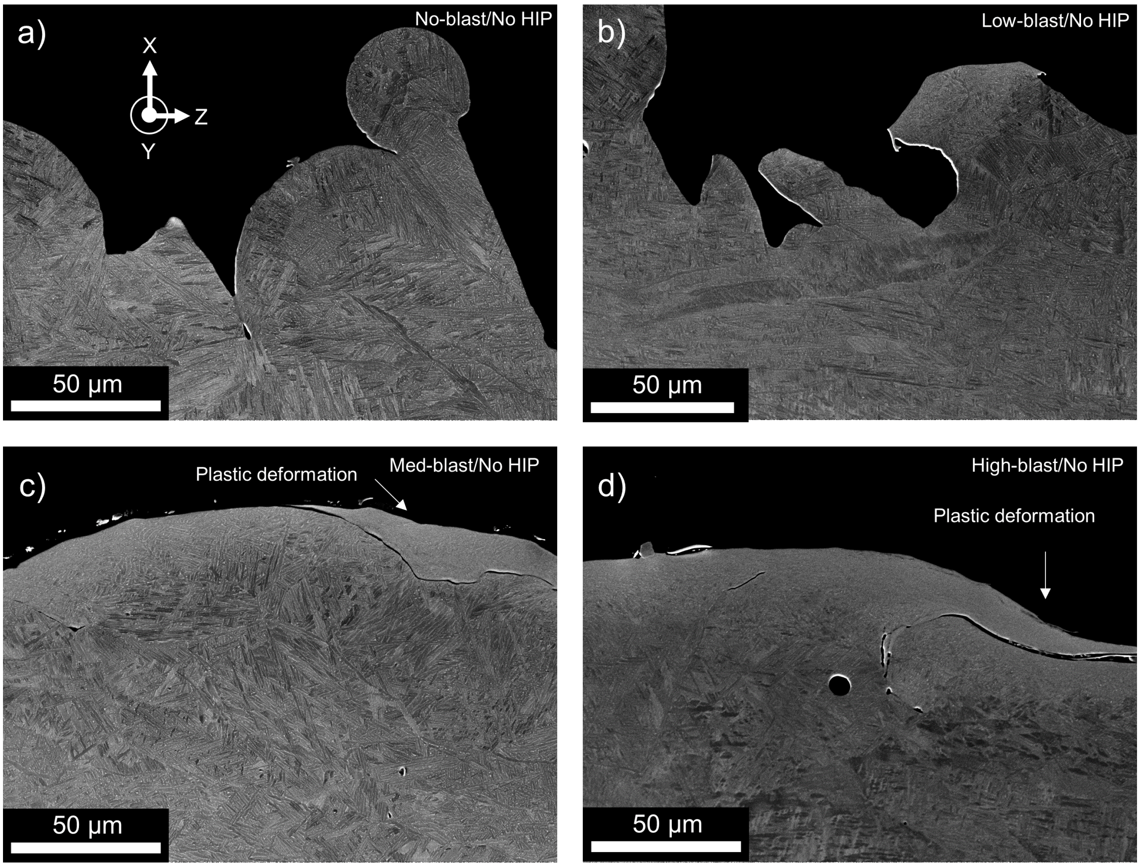

Figure 2: BSE images of the as-built specimens (No HIP). a) No-blast, b) Low-blast, c) Med-blast, d) High-blast.

4. Discussion

The microstructure of the non-HIP'd specimens (Fig. 2) display surface artifacts resulting from the plastic deformation caused by blasting. These artifacts are superficially generated pores stemming from protrusions blasted down into a flatter surface morphology, as previously observed in ultrasonic shot peening of the surface defects [9]. Although a plastic deformation zone was observed in all non-HIP'd conditions with blasting, there were no microstructural changes that occurred anywhere within the field of view for each of the specimens (Fig. 2). For the HIP specimens, there was a globular α recrystallization present at the surface that were in direct line-of-sight of the blasting, as well as a general coarsening of the Widmänstatten phase for all conditions. The No-blast/HIP specimen showed no signs of globular α recrystallization, indicating that the globular α recrystallization is the result of both blasting *and* HIP. For those that were blasted followed by HIP, the line-of-sight effect of blasting led to regions beneath protrusions that contained no globularization. The crystallographic texture for the High-blast/HIP specimen indicated that the surface became oriented in the $\{0001\}_\alpha$ direction (Fig. 4).

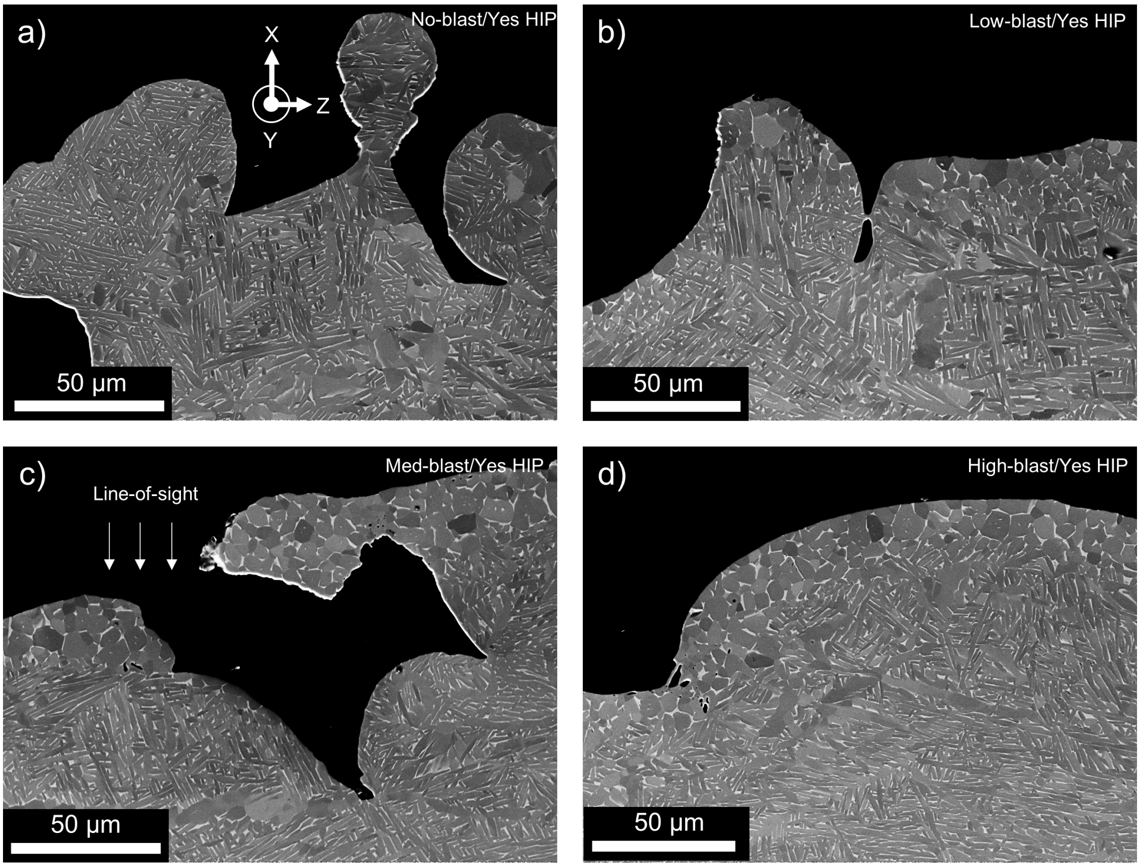

Figure 3: BSE images of the HIP'd specimens. a) No-blast, b) Low-blast, c) Med-blast, d) High-blast.

Warwick et al. show that Widmänstatten microstructure was achieved in wrought Ti-6Al-4V after hot rolling, followed by globularization taking place after heat treatments at 950 °C [10]. Stefansson and Semiatin [11] state that the globularization of Ti-6Al-4V occurs in two stages: deformation induced α-lath boundary splitting and spheroidization during initial annealing [12], followed by heat treatment induced coarsening via fault migration and Ostwald ripening [13]. We posit that the deformation from powder/part removal blasting and the common HIP/heat treatments applied to PBF-EB Ti-6Al-4V yield the same microstructural evolution at the surface with no extra processing steps.

The implications of this work are that there is likely a globular α recrystallization on *all* PBF-EB Ti-6Al-4V net shape surfaces that have undergone powder blasting and HIP. Current industrial practice does not control powder removal blasting conditions, but the results of this work suggest globular surface layer thickness can be tuned if blasting conditions are controlled. Future studies are planned to determine how the globular surface layer thickness affects the fatigue and wear properties to enable PBF-EB Ti-6Al-4V component performance tunability.

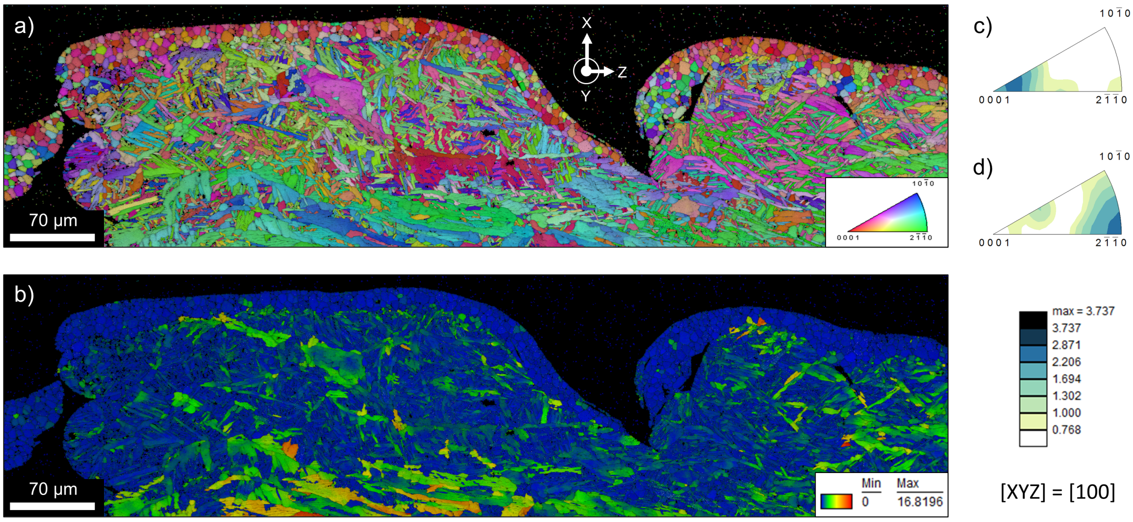

Figure 4: High-blast, HIP'd condition EBSD characterization. a) inverse pole figure map, b) GROD map, c) inverse pole figure of the surface globular phase, d) inverse pole figure of the bulk phase. IPFs were taken with the beam parallel to the X (blasting) direction [100].

5. Conclusion

It was found that a surface globular surface α recrystallization occurs during normal PBF-EB part recovery followed by HIP. The globular surface thickness increases with increasing blasting intensity. The results indicate that this globular surface may be present for all net-shape Ti-6Al-4V components manufactured via PBF-EB and subjected to HIP.

References

[1] W. S. Harun, N. S. Manam, M. S. Kamariah, S. Sharif, A. H. Zulkifly, I. Ahmad, H. Miura, A review of powdered additive manufacturing techniques for Ti-6al-4v biomedical applications, Powder Technology 331 (2018) 74–97.

[2] N. Hrabe, N. Barbosa, S. Daniewicz, N. Shamsaei, Findings from the NIST/ASTM Workshop on Mechanical Behavior of Additive Manufacturing Components, NIST Advanced Manufacturing Series (2016).

[3] ASTM F2924-14, Standard Specification for Additive Manufacturing Titanium-6 Aluminum-4 Vanadium with Powder Bed Fusion, ASTM Standards (2014).

[4] M. Svensson, Material Properties of EBM-Manufactured Ti-6Al-4V & Ti-6Al-4V ELI Under Raw and HIP Conditions, Arcam AB Internal Report (2009) 1–47.

[5] R. Molaei, A. Fatemi, N. Phan, Significance of hot isostatic pressing (HIP) on multiaxial deformation and fatigue behaviors of additive manufactured Ti-6Al-4V including build orientation and surface roughness effects, International Journal of Fatigue 117 (2018) 352–370.

[6] M. W. Wu, J. K. Chen, B. H. Lin, P. H. Chiang, Improved fatigue endurance ratio of additive manufactured Ti-6Al-4V lattice by hot isostatic pressing, Materials and Design 134 (2017) 163–170.

[7] J. Benzing, N. Hrabe, T. Quinn, R. White, R. Rentz, M. Ahlfors, Hot isostatic pressing (HIP) to achieve isotropic microstructure and retain as-built strength in an additive manufacturing titanium alloy (Ti-6Al-4V), Materials Letters 257 (2019) 126690.

[8] S. Kaboli, D. Goldbaum, R. R. Chromik, R. Gauvin, Electron channeling contrast imaging of plastic deformation induced by indentation in polycrystalline nickel, Microscopy and Microanalysis 19 (6) (2013) 1620–1631.

[9] T. Persenot, A. Burr, E. Plancher, J. Y. Buffière, R. Dendievel, G. Martin, Effect of ultrasonic shot peening on the surface defects of thin struts built by electron beam melting: Consequences on fatigue resistance, Additive Manufacturing 28 (2019) 821–830.

[10] J. L. Warwick, N. G. Jones, I. Bantounas, M. Preuss, D. Dye, In situ observation of texture and microstructure evolution during rolling and globularization of Ti-6Al-4V, Acta Materialia 61 (5) (2013) 1603–1615.

[11] N. Stefansson, S. L. Semiatin, Mechanisms of globularization of Ti-6Al-4V during static heat treatment, Metallurgical and Materials Transactions A: Physical Metallurgy and Materials Science 34 A (3) (2003) 691–698.

[12] S. Zherebtsov, M. Murzinova, G. Salishchev, S. L. Semiatin, Spheroidization ofthe lamellar microstructure in Ti-6Al-4V alloy during warm deformation and annealing, Acta Materialia 59 (10) (2011) 4138–4150.

[13] Y. L. Tian, R. W. Kraft, Mechanisms of Pearlite Spheroidization,Metallurgical Transactions A 18 (8) (1987) 1403–1414.